Digital image correlation in dental materials and related research: a review

Sungsik Yoon[a], Hyung-Jo Jung[b], JC Knowles, Hae-Hyoung Lee[c,*]

[a]*Department of Civil and Environmental Engineering, University of Illinois at Urbana-Champaign, Urbana, IL 61801, USA*

[b]*Department of Civil and Environmental Engineering, Korea Advanced Institute of Science and Technology, Daejeon 34141, Republic of Korea*

[c]*Department of Biomaterials Science, College of Dentistry, Dankook University, Cheonan 31116, Republic of Korea*

*Corresponding author

E-mail: haelee@dku.edu, Tel.: +82 41 550 1925

Abstract:

Keywords: Digital image correlation, dental materials, mechanical properties, shrinkage behavior, Implant-supported material, prosthesis load transfer

---

1. Introduction

Various instruments and techniques have been used to accurately measure deformation not only in engineering but also for materials or tissues in the biomechanical field, and these methods include strain gauging, linear variable differential transformer (LVDT), and fiber bragg grating sensors (FBGS) [1-4]. However, these conventional measuring methods have the disadvantage that they are expensive and cannot be handled easily, in particular, the response of the material is significantly affected by external environmental variables such as temperature and moisture conditions. Moreover, LVDTs and strain gauges require manual sensor attachment and only the response values of the gauge points can be obtained, making it difficult to evaluate the whole mechanical behaviors. Especially for biomaterials, it is essential to evaluate the entire displacement field to predict accurate material behavior, because most of the biomaterials have not only anisotropic properties with complex shapes but also heterogeneous material behavior [5].

In order to overcome the limitations of conventional measuring methods, various optical measurement techniques have recently been developed based on optical imaging. Image-based measurement algorithms were actively developed stemming fromphotogrammetry in the 1980s, and attracted attention in industry and research as they were first applied to mechanical testing in the 1990s [6-8]. In particular, optical measurement techniques have substantial advantages over conventional measurement methods such as automation, consistency, and non-contact, so it is widely utilized in various fields including engineering, biomechanics, medical fields, and etc. [5, 9].

- **Automation**: Easily configured processes for automatically acquiring and analyzing images without the need for complicated equipment and materials. This enables the

evaluation and prediction of the behavior of biomaterials with entire displacement fields calculated in real-time.

- **Consistency:** Conventional attachable gauges can have different sensitivity depending on laboratory environments such as temperature and humidity. However, because image-based measurement systems are not affected by the environments, the researcher can obtain consistent experimental results regardless of field conditions.

- **Non-contact:** The optical measuring system can measure the displacement field without attaching a gauge to the specimen (without access to the specimen). Especially in deformable biomaterials such as soft tissues, the deformation fields can be easily obtained without disturbing the specimen.

In order to predict an accurate displacement field, it is necessary to consider the appropriate optical technology for the purpose of the experiments. For example, hologram interferometry, speckle interferometry, and electronic speckle pattern interferometry techniques are sensitive to small displacements, and therefore are not suitable for deformable materials such as soft tissues [10]. Similarly, moire interferometers are not suitable for irregularly shaped biomaterials, as they must apply a regular pattern to the sample specimen surface. [11].

Digital image correlation (DIC) technique has gained widespread attention as an experimental method that not only has the advantages of conventional optical measurement but also overcomes the existing limitations [8]. DIC is a non-contact measurement method that allows evaluation of the entire deformation field of regions of interest (ROI) by comparing a grayscale image before and after deformation. DIC technology began to be developed in the early 2000s,

based on the field of engineering, and has gradually been applied to various biomechanical areas.

It was initially applied to hard tissues, such as bone, and its application gradually expanded to soft tissues. For hard tissue level, McKinley and Bay [12] and Cyganik et al. [13] evaluated the displacement and strain distribution of trabecular bone of humans through uniaxial compression experiments. Palanca et al. [14] utilized texture correlation to measure the strain distribution of the vertebral body section and Mann et al. [15] assessed the micro interfacial displacement of the cement-bone interface by employing shear fatigue tests. In addition, major principal strains, principal minimum strains, and displacement distributions were measured using various bone materials such as human femurs [16-18], hemi-pelvis [19, 20], and spine [21]. Even for soft tissue analysis, extensometers were mainly utilized to measure the strain of discrete points. However, because the gauge had to be installed in soft tissue surface, it was verydifficul to observe the exact deformation of the specimen with low stiffness material [22]. Moreover, Brunon et al. [23] measured displacement and strain distribution of human liver by inflation test, and Elliott et al. [24] measured the axial and lateral strain of human cartilage and cervical tissue by tensile test. Furthermore, DIC techniques were also utilized to measure deformations of soft tissue such as human eyes [25], tendons (ligament) [26, 27], and keratinized tissue [28, 29].

Dental restorations have to withstand static or repetitive masticatory loading during use in the mouth. In the oral cavity, mastication generated occlusal forces range from 400 N to 800 N for healthy people in various directions causing deformation of teeth and the related tissue structure and restorative materials [30]. Therefore, accurate and precise measurement of strain plays an important role for predicting the mechanical behavior and for measuring the mechanical properties of dental restorative materials. Moreover, DIC technologies are more attractive to those fields

which are constructed with layering of hard and soft dental tissues combined with various types of restorative or prosthetic materials. In particular, it can be applied to various materials and experiments such as measuring strain of dental restorative and prosthetic materials under loading and evaluating their mechanical behavior. Although the DIC techniques were applied in dentistry later than in biomedical field, these techniques are in the limelight recently as a way to replace traditional measuring methods. Therefore, it is important to summarize and present the advantages and disadvantages of the experimental methods applied to dental materials by using DIC technique.

Previous review papers on the applications of DIC technology have been focused only on the biomechanical issues with no in-depth discussion on the theoretical explanation and speckle pattern issues of DIC technology. This paper discusses in detail the basic principles of DIC techniques, image matching algorithms and random speckle patterns that can overcome the limitations of other optical methods. In particular, we will focus on reviewing the application of the methodology in the dental materials and related fields. For this reason, this review focuses the application cases of DIC technique in the dental materials and related fields with discussion of future technology development such as 3-D DIC techniques. In addition, we will clearly distinguish the strengths and limitations of the DIC technique applied in the dental research field and propose future development directions to overcome them.

2. Principles of Digital Image Correlation Techniques

The application of DIC techniques is simple and easy to use regardless of the specimen

type and size of the material, so it has shown continued and increased interest in many research fields [31-33]. For this reason, many DIC algorithms have been developed based on the engineering domain, and it has been utilized as a verification tool in various laboratory-scale tests and field experiments.

2.1 Principles of DIC Techniques

DIC is a non-contact experimental method that stores images of material surfaces in digital form. The basic principles of DIC method is to find an image correlation between the reference image and deformed images with respect to different load levels [34]. For image correlation, digital images can be stored to measure the displacement field within the region of interest based on the grayscale (0-255) similarity [8]. Thus, white paint is generally applied to the surface of the material, and black paint is used to form any random speckle pattern (spot pattern). The surrounding white light is also utilized to increase the contrast between foreground and background intensity due to speckle pattern randomness. Fig. 1 shows a set of workflows and a typical experimental setup for a 2-D DIC device that obtains material surface displacement and strain fields through DIC technology [18]. To obtain the in-plane displacement fields, only a single camera should be used, but more than two cameras are needed to obtain the out-of-plane displacement field. A detailed description of image matching algorithm and random speckle pattern is explained in the next section.

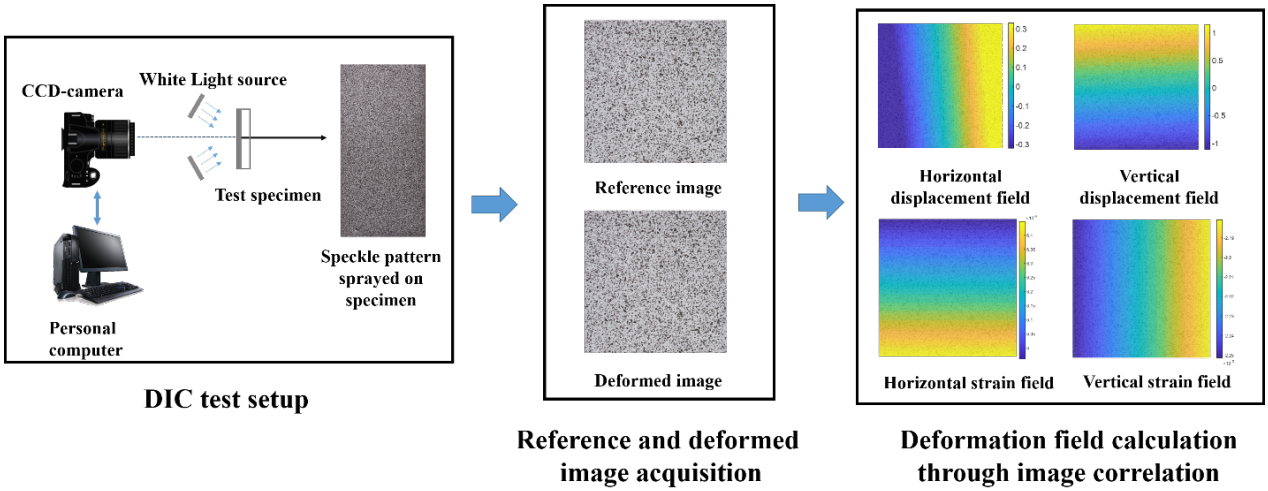

Fig.1 Principles of digital image correlation (DIC) algorithm and generalized experimental setup permission?

2.2 Image Correlation Algorithms

Numerous image correlation algorithms for obtaining the displacement field have been continuously developed, including the Lucas-Kanade tracking algorithm [34], the subset shape function algorithm [31, 35], and Full-field algorithm [36, 37]. Thus, in-plane displacement on specimen surface can be extracted using iterative algorithms, e.g., Newton-Raphson method [38] and Levenberg-Marquardt method [37]. However, because the Lucas-Kanade algorithm has low tracking accuracy when excessive deformation occurs, the subset function algorithm or the full file algorithm is mainly used. The subset function algorithm divides the image ROI into the same subset to represent image correlation coefficient. Full-field algorithms, on the other hand, represent a technique for correlating images by setting the entire image to ROI before and after deformation. The principle of the two algorithms is the same, and the results have been verified in previous research, so they tend to be utilized mainly for experimental purposes and for user convenience.

For correlating the two images (i.e., between reference and deformed images), the whole images should be divided into sub-images (subset) and an image matching algorithm obtain a displacement field for each subset. Since the correlation ROI varies depending on the position and size of the subset, it is necessary to determine the appropriate subset according to the state of the specimen undergoing deformation. Fig. 2 shows reference image and deformed image after load is applied. Generally, each subset is composed of the (2*m*+1) by (2*m*+1) pixels, where *m* is integer number. If the grid point of the subset of images before deformation is (*x*, *y*) and the grid point of the corresponding image subset after deformation is (*x′*, *y′*), as shown in Fig. 2, then the displacement field of each subset can be represented as a relationship.

$$x' = x + u$$

$$y' = y + v$$

where *u* represents horizontal displacement, *v* represent vertical displacement, and (*x*, *y*) and (*x′*, *y′*) are the subset center point coordinates before and after deformation, respectively. Each deformation field can be approximated with displacement, the first derivative of displacement, and second derivative of displacement by employing a second-order Taylor series expansion. The displacement fields *u* and *v* obtained from the second-order Taylor series expansion are expressed as follows [9]:

$$u = u_0 + \frac{\partial u}{\partial x}\Delta x + \frac{\partial u}{\partial y}\Delta y + \frac{1}{2}\frac{\partial^2 u}{\partial x^2}\Delta x^2 + \frac{1}{2}\frac{\partial^2 u}{\partial y^2}\Delta y^2 + \frac{1}{2}\frac{\partial^2 u}{\partial x \partial y}\Delta x \Delta y$$

$$v = v_0 + \frac{\partial v}{\partial x}\Delta x + \frac{\partial v}{\partial y}\Delta y + \frac{1}{2}\frac{\partial^2 v}{\partial x^2}\Delta x^2 + \frac{1}{2}\frac{\partial^2 v}{\partial y^2}\Delta y^2 + \frac{1}{2}\frac{\partial^2 v}{\partial x \partial y}\Delta x \Delta y$$

where u_0 and v_0 represent the rigid body motion, and remaining terms represent the first-order displacement (strain term) and second-order displacement of the before deformation subset (x, y), respectively. In order to evaluate deformation of each subset, the displacement field can be evaluated by minimizing the difference between the gray-intensity distributions of the subset grid point (x, y) and (x', y'). The equation for minimizing the correlation coefficient of each subset can be expressed as:

$$\min C = \frac{\sum_{\Omega}\{I_r(x,y) - I_d(x',y',\Psi)\}^2}{\sum_{\Omega} I_i(x,y)^2}$$

where Ω represents the entire domain of the ROI, $I_r(x,y)$ is the gray-intensity distribution of the reference subset, $I_d(x',y',\Psi)$ is the gray-intensity distribution of deformed subset, and Ψ is displacement information obtained from second-order Taylor series expansion. To minimize the correlation coefficient, iterative calculations, such as the Newton-Raphson method, is required until the derivative C is converged or the displacement information Ψ converges. Based on the optical behavior, it is assumed that the brightness of the initial subset and deformed subset is the same.

$$I_r(x,y,t) = I_d(x+\Delta x, y+\Delta y, t+\Delta t)$$

where (x, y, z) is the coordinates of the initial state subset at time t and (Δx, Δy) is the magnitude of displacement in each direction after deformation during the time increment (Δt).

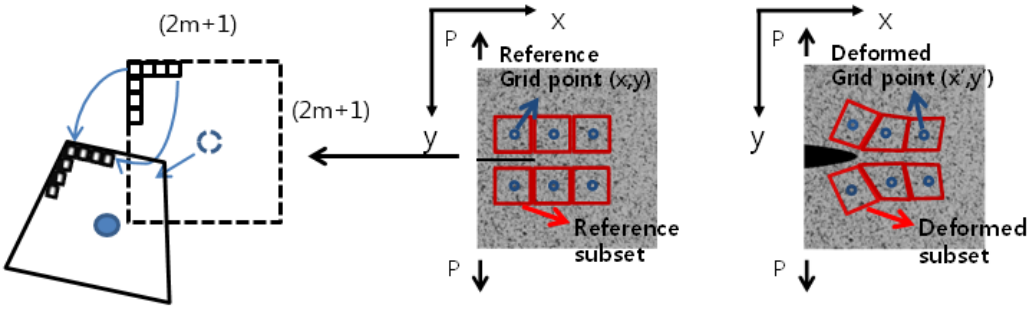

Fig.2 Schematic illustration of image matching algorithm for digital image correlation

2.3 Random Speckle Patterns

The accuracy of image correlation shows a tendency to depend on the gray intensity distribution of the image before and after deformation. Therefore, the accuracy of the image matching algorithm can be influenced by light changes, specimen conditions, camera conditions, and the shape of random speckle patterns [9]. Although most of the experimental environments are similar, the most influential factor is known as the gray-intensity according to the random speckle pattern. That is, the distribution of perfect white color (gray-intensity: 0) and a perfect black color (gray-intensity: 255) should be generated randomly. Decreasing the randomness of the speckle pattern can result in similar subsets of the pattern, which reduces the accuracy of image correlation before and after deformation. Thus, in order to increase the local uniqueness of the speckle pattern, generally white paint is sprayed onto the surface of the test material, and after it is completely dried, the speckle pattern is formed using black paint using an air spray. The speckle pattern is generated differently depending on the air spray nozzle and pressure. According to the literature, the generation of speckle patterns is determined by user experience and skill [9].

Fig. 3 shows the gray intensity distribution for a specific subset of specimens in which open mode occurs. In each subset, the mean gray intensity values are 169 and 149, with standard deviations of 42 and 40. As such, when the gray-intensity distribution including the mean and the standard deviation of the subset has a large randomness, a result with high correlation accuracy can be obtained.

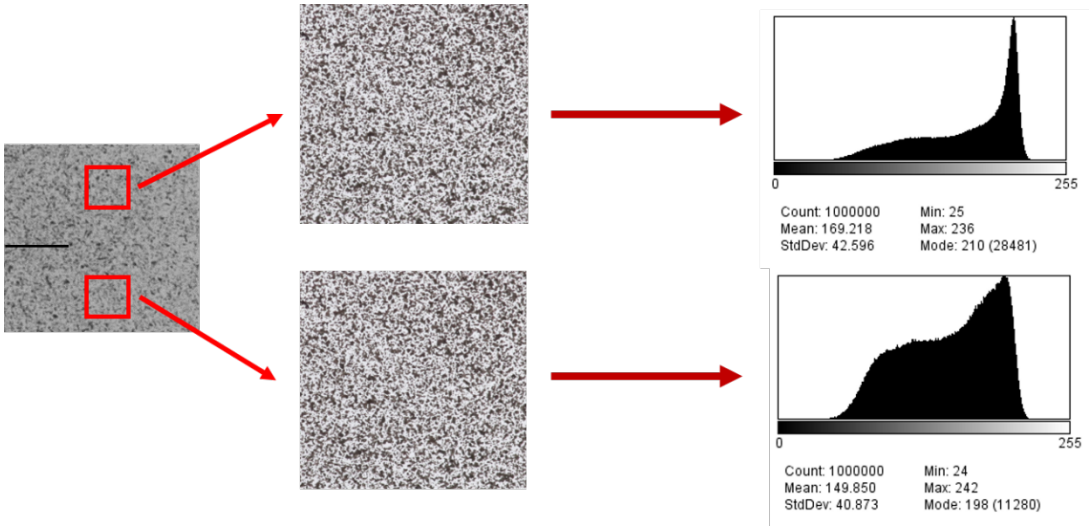

Fig. 3. Example of randomly generated speckle patterns (Park et al. 2017) permission?

3 Application to dental materials and related field

3.1 Shrinkage behavior of light-cured dental resin composites

Polymerization shrinkage of light-cured dental resin composites with resulting contraction stresses has known to be one of the causes for reduced clinical outcome success of those restorations, due to deleterious effects on the integrity of resin-tooth interfaces and mechanical properties of the materials themselves [39, 40]. Thus, a wide variety of method or techniques have been

developedand applied to the measurement of polymerization contraction shrinkage resulting from light-curing of light-cured dental resin composites, using linear (linometer) [41-43] or volumetric shrinkage test systems [44-47].

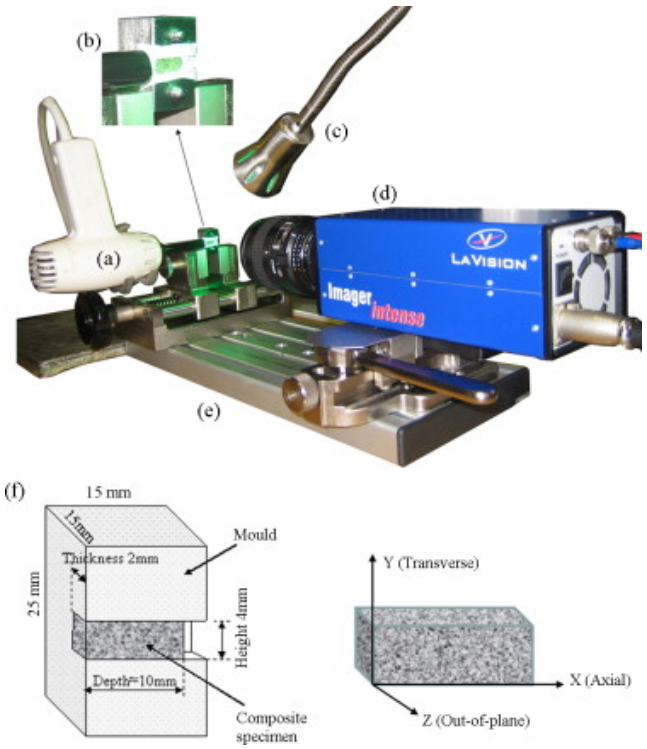

Fig. 4 Polymerization shrinkage of dental composites (Li et al. 2009) with permission

A digital image correlation test setup using a CCD camera was firstly used to measure the polymerization shrinkage of dental composites in a simulated cavity by Chuang et al. [48]. They also demonstrated the DIC technique was able to measure the displacement of specific locations in dental restorations and to provide a bridge to connect computer simulation data. Strain values measured by the DIC method were found to be very close to that measured by strain gauge method, demonstrating the accuracy of DIC measurement [49]. Li et al. measured the full-field polymerization shrinkage of dental composites using optical image correlation method. For the

experiment, curing conditions were adjusted through different irradiance levels, and images were acquired at 0.1 Hz intervals for 30 minutes using a single camera (Fig. 4). These results showed that the DIC method is suitable for generating full-field displacement information on polymerization shrinkage behavior of dental composites when compared to other measurement tools. In addition, Li et al. [50, 51] adopted the DIC technique to measure the full-field stress and strain distributions of dental resin composites during polymerization shrinkage. Experimental results showed that the resin composite exhibited significant shrinkage strain in the vertical direction of the cavity, with the largest downward displacement at the center of the restoration. In addition, relatively uniform strain occurred around the restoration, and the extent was consistent with the volumetric shrinkage deformation of the material. The volumetric shrinkage of material can be assumed to be three times that of the linear shrinkage determined by a linometer or DIC method [41, 44, 49]. It has been shown that the volumetric shrinkage value measured by DIC technique was comparable with that measured by a linometer system [42, 49], but was lower than that measured by mercury dilatometer [52]. Furthermore, Li et al. [53] employs the DIC technique to measure temporal variations of material properties of dental composites during polymerization. In their study, multiple correlations of dental composite properties were investigated for the correlation of Knoop hardness, elastic modulus, viscosity, and polymerization shrinkage based on the hysteresis curve of polymerization shrinkage-strain. The measured correlation can be applied to other dental composites, so it can be used as important basic data.

The key advantages of the DIC technique was to understand the shrinkage behavior of light-cured composite resins in near clinical situation. Thus, in such case, the non-contact full-field DIC technique can be capable of measuring surface strain at any position throughout the material and

in-situ shrinkage behavior of composite restorations in the tooth cavity [49]. Chuang et al. used DIC to measure the spatial and temporal deformation of resin-based composites under the different interface boundaries of the tooth restoration [54]. Moreover, in order to investigate *in situ* polymerization shrinkage of the resin composites according to the tooth cavity geometry and used it as a tool for validation of computational finite element methods (FEA) (Fig. 5) [55]. They also studied the shrinkage behaviors, shrinkage stress, and microleakage of composite restorations under the different light-curing protocol, a DIC technique was combined with the FEA results [56, 57]. The experimental results showed that the intensity and direction of light influenced the shrinkage and contraction of composite resin, and the degree of shrinkage strain and stress tended to decrease with an oblique irradiation direction in comparison with vertical direction during curing of composite restoration [56]. These studies demonstrated that the experimental-numerical hybrid technique can be used as a comprehensive and definite tool to analysis stress developments in restorative dentistry

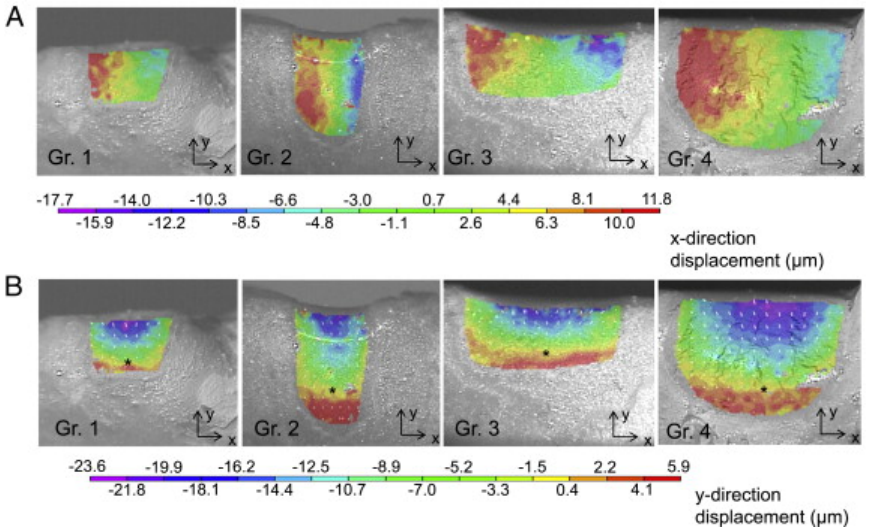

Fig. 5 Polymerization shrinkage of dental composites (Chung et al. 2011)

Lau et al. [58] investigated the full-field polymerization shrinkage of dental resin composites as a function of time and position by inversely synchronized camera's shutter in real time. In order to obtain an image, the maximum strain was measured in real-time by adjusting the camera shutter and image time, and the shrinkage strain kinetics of the dental resin was assessed as a function of the depth of the specimen. Novaes Jr et al. [59] utilized DIC to measure superficial shrinkage displacement and then detected debonding of the subsurface of the resin composite restoration. The measurement results (debonding at the pulpal floor) were compared with theoretical results based on material mechanics. The significant finding of this experiment was that interfacial debonding of restoration can be predicted from the difference between the measured and expected surface displacement of composite resin restoration. The above studies showed that the DIC technique can be effectively used to measure the polymerization shrinkage kinetics of restorations with different boundaries [57].

Further, it has been demonstrated by using a 3D DIC analysis system using two cameras in a clinically relevant configuration that polymerization shrinkage of dental composite resins will not occur evenly throughout specimens and at the adhesive interface [60, 61]. Miletic et al. conducted the 3D DIC analysis to measure the strain and displacement distributions of various resin composites and the amount of axial and gingival microleakage along the resin-dentin interface in a modified class II cavities of human teeth [62].

3.2 Mechanical behavior of dental composite interface

Research has been carried out to understand the interfacial behavior between dentin and dental composites and to predict the bond strength. ~~*Reducing the bonding strength of the dentin can lead to continuous failures, so it is important to accurately predict bonding strength and identify degradation.*~~ Huang et al. [63] evaluated dentin bonding strength with a modified Brazilian disk test to predict failure of dental restorations. In their research, the DIC technique allowed them to accurately predict the actual stress-strain distribution and capture the fracture process in real-time. Through their experimental methods, the bond and tensile strength of the four resin composites were evaluated. Similarly, Carrera et al. [64] predicted the bond strength of dentin composites using the Brazilian disk test. Acoustic emission (AE) and DIC techniques were utilized to monitor the debonding of the composite, and the mean bond strengths were measured for different three adhesives. In addition, Li et al. [65] assessed the mechanical behavior at the dentin-composite interface when degradation of dental composite restorations occurred (due to multiple oral biofilms). In these studies, the DIC technique was effectively used to obtain the strain mapping from the images of the stressed composite resin surfaces.

3.3 Evaluation of mechanical properties of tooth structure

Prior to determining the mechanical properties of a small object like tooth structure, it is very important measuring the strain value precisely and for that, optical imaging technique (DIC) can be valuable tool [3]. The initial approach using DIC technology was applied to measuring the compressive elastic properties from a very small piece of dentin in a rectangular or cylindrical form (1.5x1.0x1.0 mm or 2.1 mm in diameter). Palamara generated 43 regular grids on the

specimen surface to measure the compressive strain value of the dentin piece [66]. Wang et al. [67] has proposed a method to measure the mechanical properties of dentin by combining Finite Element Analysis (FEA) and the DIC technique. The proposed methodology validates the results from the three-point bending test and the four-point bending test in comparison with previous studies.

Zhang et al. [68] quantified dimensional changes during dehydration using dentin and enamel in young and elderly patients. Microscopic DIC was used to measure the deformation of dentin and enamel, and specimens were prepared according to the patient's age, dentin tubules, and enamel prism orientation. The strain distribution was calculated during dehydration and the effective dehydration coefficient was estimated. Experimental results show that shrinkage deformation is greater in dentin than enamel. The microscopic DIC was also very useful to identify the crack tip in human or elephant dentin structures complexed with their tubular structure using a stereomicroscope [69, 70]. Those systems for the microscopic DIC analysis are described elsewhere [71].

There has been an approach to elucidate mechanical behavior of dentin at the micro or nano-scale using image tools combined with the DIC technique. Sui et al. [72] evaluated the residual elastic strain over the human dentine-enamel junction (DEJ) using a novel focused ion beam milling with DIC techniques technique. The proposed new method is useful for understanding DEJ behavior at the micrometer scale and has significant impacts on the development of improved biomimetic materials. In particular, the accurate measurement of microscale strain in the dentin interface region is crucial because it can be a performance indicator for predicting overall dental condition. Using this approach, residual strain existing at the

interfaces between porcelain veneer and zirconia ceramic core can be quantified [73]. Another example of the combined methodology was conducted by an application of digital volume correlation (DVC) to X-ray nano-CT image of elephant tusk [74]. However, although DVC can be a 3D analogue of DIC, some technical problems (noise effects, long acquisition time for image data) should be improved before further application to internal strain measurement [2].

3.4 Evaluation of fracture characteristic of dental restorative materials

When the deformation of the dental material reaches the ultimate state, a fracture or rupture occurs, which leads to more serious damage. After the initial use of imaging techniques for measuring surface strain in human dentin by Palamara et al [66]., Zhang et al. [75] developed a special compact tension specimen of human dentin. Further, they utilized the microscopic DIC method to examine crack opening displacement distribution (Mode I) to investigate the crack growth resistance mechanism in human dentin, which enables prediction of the stress intensity factor and crack growth at the crack tip of the dentin and enamel junctions. After this, Zhang et al. [76] evaluated the fracture mode and initiation mechanism of dental all-ceramic crowns under monotonic Hertzian contact load using both flat and curved occlusal specimens. In particular, the critical loads at the time of crack initiation were calculated and crack propagation behavior in the ceramic materials were also investigated using the full-field DIC technique as a function of loading. Results of the experiment confirmed that the debonding failure at core-tooth interface initiated at substantially lower loads than those of crown fracture, highlighting the importance of dental cements and tooth preparations for successful dental ceramic crowns.

Jiang et al. [77] and Porto et al. [78] utilized full-field stain maps provided by DIC to measure the J-integrals and the fracture toughness of dental restorative ceramics and composites. Moreover, Sebastiani et al. [79] measured the residual micro-stress distribution of heat-pressed ceramic on zirconia and porcelain-fused to metal systems and evaluated fracture toughness based on the measured strain distribution.

The DIC technique has been little utilized in the measurement of mechanical properties of dental restoratives or prosthetic materials in bulk form, possibly due to the need for the additional equipment setup and complex interpretation work. Chen et al. [80] measured the deformation of a rectangular piezoelectric ceramic (lead zirconate titanate) blocks (5 x 5 x 15 mm^3) under uniaxial compressive loading. In their research, a barrel behavior was demonstrated by calculating the strain distribution on the selected ROI area. Their results further indicated that the ROI and aspect ratio of specimens should be considered to obtain the true strain results under compressive load. Recently, Choi et al. [81] evaluated the elastic modulus and Poisson's ratio of the CAD-CAM resin-composite block materials using the DIC setup appeared in Fig. 1. The modulus of elasticity obtained from the DIC were compared with the results of the uniaxial beam, biaxial disk flexure test and compression test. The experimental results showed that the DIC results are in good agreement with the results of a typical uniaxial three-point flexural test (span to height ratio of 10). The elastic modulus values determined by the load-displacement data from compression testing machine were generally underestimated by those from the DIC technique, particularly for high-stiffness materials. The DIC technique can be applied to the measurement of macroscopic material properties for the purpose of securing precision.

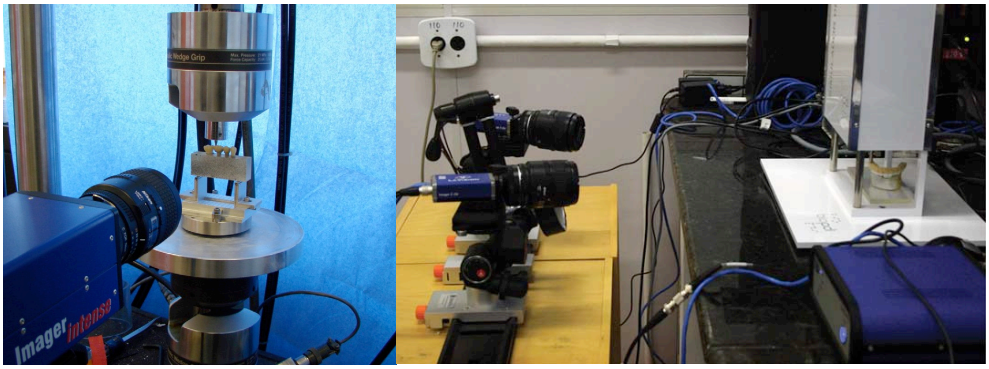

Fig. 6A 6B

Tiossi 2011, 2017)

3.5 Deformation of dental restoration and Implant-supported prosthesis

Full-field DIC methodology is a highly efficient system capable of providing in situ displacement of complex geometry dental restorations and prostheses supported by implants including the surrounding bony structure. Ni et al. [82] adopted the optical method to measure the amount of displacement of endodontically restored teeth with posts when they were loaded with a 100 N. The results were used to interpret the effect of different post materials (glass-fiber, titanium, and cast metal post) with related parameters on the marginal integrity and root fracture resistance. Tiossi et al. [83, 84] studied the influence of splinting design or crown materials with different stiffness on the bone strain distribution surrounding implant-supported prosthesis embedded in PMMA block (Fig. 6A). For this purpose, screw-retained splinted crowns were fabricated using porcelain-veneer

and resin-veneer, and the surface deformation of the bone block was measured depending on the use of crown materials and second molar. For image acquisition, images were taken at a rate of 1.0 Hz while applying a force up to about 250 N. Experiments have shown that the use of soft resin veneer materials can evenly distribute the load on the supporting teeth and implants, further reducing bone deformation. The in-plane strains measured were significant dependent on the splinting design of prosthesis.

After this, Tiossi et al. utilized a photoelastic model [85] and a finite element model [86] to predict bone-strain induced from implant-supported prostheses and verified the results using DIC techniques. The first premolar and second molar together with threaded implants were manufactured using acrylic resin replicas, and splinted and non-splinted metal-ceramic screw-retained crowns were fabricated. The strains calculated at the implant-resin interface using FE models were much higher than the surface strain by DIC. The results therefore indicated that the capability of providing surface strains only can be a limitation of DIC method [87]. Although DIC is slightly less sensitive than the photoelastic method [85], however, DIC can validate the FE models (Fig. 7) [86] .

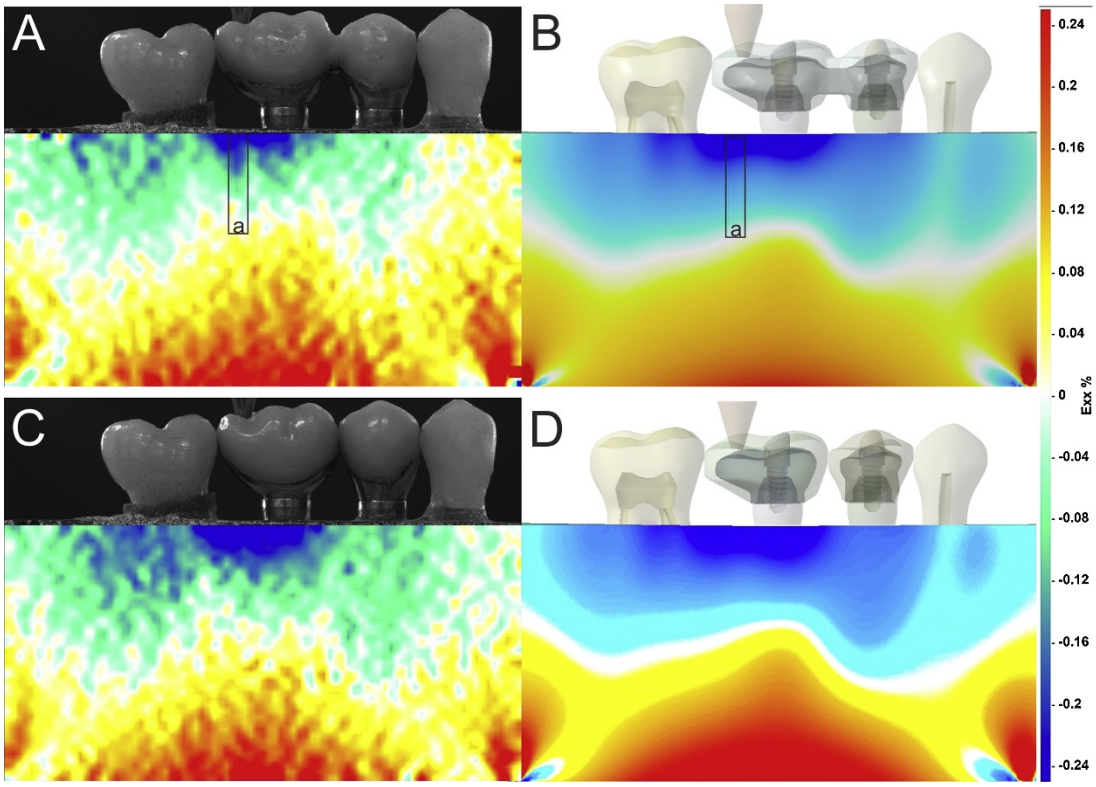

Fig. 7 Tossi et al. 2013 Dent Mater with permission

Another limitation of the conventional two-dimensional DIC technology is that only in-plane deformation can be measured when a single camera is used [88]. For this purpose, in recent years, the 2D DIC is extended to three-dimensional digital image correlation (3D DIC) technique through two cameras which can allow for measuring the spatial deformation and visualization of the target material [89] (Fig. 6B). Using the 3D DIC technique, Tanasic et al. [90, 91] successively analyzed the compressive strain below the removable and fixed prosthesis in a donated human mandible using a commercial 3D DIC system (GOM, Germany). Experimental results showed that the removable partial denture model had a higher strain than the fixed partial denture model, and the strain was concentrated in the alveolar bone around the abutment teeth. Moreover, Tiossi et al. [89] investigated the biomechanical behavior of implant-supported full arch fixed dental

prostheses (FAFDP) according to the titanium and zirconia framework. For this purpose, 14-unit FAFDPs (supported by 6 implants) and 12-unit FAFDPs (supported by 4 implants) were tested, and deformation of specimen surface was measured by DIC when a 250 N single-point load was applied to the second premolar. Experimental results showed that higher strains were detected in Zirconia frameworks and FAFDPs supported by 4 implants.

Clelland et al. [92] utilized 3D DIC technique to measure bone deformation induced by cement and screw-retained implant prostheses under different oblique and vertical loads using a commercial image correlation software (Vic-3D, USA). Calha et al. [93] evaluated the effects of deformation on the geometry of anterior implant-supported zirconia using two high-speed cameras and image correlation system. Four-unit zirconia implant abutments were prepared using CAD/CAM materials and fabricated in two experimental groups according to the straight and curved shape. The image was acquired using a high-speed camera while the load was up to 200N, and the three-dimensional deformation map in the was rendered using a video correlation system. Experimental results show that the geometry affects the anterior implant-supported zirconia and that larger deformations occur in the curved specimens. Yilmaz et al. [94] and Clelland et al. [95] investigated the strain induced by splinted and non-splinted cement-retained implant crowns. The 3-D DIC method was applied to measure the strain of the crown when the 400N load was applied in the vertical and oblique directions. The experimental results showed that splinting has a minimal effect on load sharing between adjacent cement-retained crowns. They also compared the displacement of CAD/CAM titanium and zirconia abutments with different internal connections using 3D DIC [96]. The three-dimensional DIC technique was employed to measure the displacement of the abutments, and larger strains were observed on specimens requiring higher

torque. Further studies utilized 3D DIC to conduct analysis in strain transfer behavior of various implant abutment design and treatment options [97, 98]. Overall these researches demonstrate that the 3D DIC technique using two-camera system is useful for measuring the out-plane surface strains of removable and fixed prosthesis and bone surfaces with enhanced accuracy.

5 Conclusion

The DIC techniques have gained great interest as a potential tool for dental materials and related research. The scope of this review is to briefly explain the principles and algorithms of DIC, and to review the case studies of DIC technology in dental materials and restorations in five categories: polymerization shrinkage and interface behavior of light-cured dental composite resins, evaluation of mechanical properties of tooth structure, fracture characteristic of dental restorative materials, and deformation of dental restoration and Implant-supported prosthesis.

This review paper demonstrates the potential usefulness of DIC technology as a 2D and 3D strain measurement tool for dental materials and restorations. the versatility of the DIC technique can be extended by combining DIC with other measurement techniques, such as FEA or Micro-CT. Further, strain distribution of dental restorations and prosthesis under occlusal loading can be visualized and measured in/ex vivo and in situ by 3D DIC technology. However, special care for specimen preparation, clear image acquisition, and appropriate calibration processes should be guaranteed to obtain accurate and precise measurement of deformation.

Acknowledgements

This work was supported by a National Research Foundation (NRF) grant (2020R1A2C1005867) funded by the Ministry of Science and ICT, and by the Global Research Development Center Program (2018K1A4A3A01064257) and Priority Research Center Program (2019R1A6A1A11034536) by the Ministry of Education of Korea.

References

[1] Khan AS, Wang X. Strain measurements and stress analysis: Prentice Hall NJ; 2001.
[2] Grassi L, Isaksson H. Extracting accurate strain measurements in bone mechanics: A critical review of current methods. J Mech Behav Biomed Mater. 2015;50:43-54.
[3] Zhang D, Arola D. Applications of digital image correlation to biological tissues. Journal of Biomedical Optics. 2004;9.
[4] Fresvig T, Ludvigsen P, Steen H, Reikerås O. Fibre optic Bragg grating sensors: an alternative method to strain gauges for measuring deformation in bone. Medical engineering & physics. 2008;30:104-8.
[5] Palanca M, Tozzi G, Cristofolini L. The use of digital image correlation in the biomechanical area: a review. International Biomechanics. 2016;3:1-21.
[6] Sutton MA, Wolters WJ, Peters WH, Ranson WF, McNeill SR. Determination of displacements using an improved digital correlation method. Image and Vision Computing. 1983;1:133-9.
[7] Sutton MA, Mingqi C, Peters WH, Chao YJ, McNeill SR. Application of an optimized digital correlation method to planar deformation analysis. Image and Vision Computing. 1986;4:143-50.
[8] Sutton MA, Orteu JJ, Schreier HW. Image correlation for shape, motion and deformation meaasurements. New York: Springer Science; 2009.
[9] Park J, Yoon S, Kwon T-H, Park K. Assessment of speckle-pattern quality in digital image correlation based on gray intensity and speckle morphology. Optics and Lasers in Engineering. 2017;91:62-72.
[10] Freddi A, Olmi G, Cristofolini L. Experimental stress analysis for materials and structures. Stress analysis models for developing design methodologies Series in solid and structural mechanics. 2015;1.
[11] Post D. Moiré interferometry: advances and applications. Experimental Mechanics. 1991;31:276-80.

[12] McKinley TO, Bay BK. Trabecular bone strain changes associated with subchondral stiffening of the proximal tibia. Journal of biomechanics. 2003;36:155-63.
[13] Cyganik Ł, Binkowski M, Kokot G, Rusin T, Popik P, Bolechała F, et al. Prediction of Young′ s modulus of trabeculae in microscale using macro-scale′ s relationships between bone density and mechanical properties. Journal of the mechanical behavior of biomedical materials. 2014;36:120-34.
[14] Palanca M, Brugo TM, Cristofolini L. Use of digital image correlation to investigate the biomechanics of the vertebra. Journal of Mechanics in Medicine and Biology. 2015;15:1540004.
[15] Mann KA, Miller MA, Cleary RJ, Janssen D, Verdonschot N. Experimental micromechanics of the cement–bone interface. Journal of orthopaedic research. 2008;26:872-9.
[16] Op Den Buijs J, Dragomir-Daescu D. Validated finite element models of the proximal femur using two-dimensional projected geometry and bone density. Computer Methods and Programs in Biomedicine. 2011;104:168-74.
[17] Helgason B, S.Gilchrist, Ariza O, Chak JD, Zheng G, Widmer RP, et al. Development of a balanced experimental–computational approach to understanding the mechanics of proximal femur fractures. Medical Engineering & Physics. 2014;36:793-9.
[18] Gilchrist S, Guy P, Cripton PA. Development of an Inertia-Driven Model of Sideways Fall for Detailed Study of Femur Fracture Mechanics. Journal of Biomechanical Engineering. 2013;135:121001--8.
[19] Ghosh R, Gupta S, Dickinson A, Browne M. Experimental Validation of Finite Element Models of Intact and Implanted Composite Hemipelvises Using Digital Image Correlation. Journal of Biomechanical Engineering. 2012;134:081003--9.
[20] Dickinson AS, Taylor AC, Browne M. The influence of acetabular cup material on pelvis cortex surface strains, measured using digital image correlation. Journal of Biomechanics. 2012;45:719-23.
[21] Ruspi ML, Palanca M, Faldini C, Cristofolini L. Full-field in vitro investigation of hard and soft tissue strain in the spine by means of Digital Image Correlation. Muscles Ligaments Tendons J. 2017;7:538-45.
[22] Disney CM, Lee PD, Hoyland JA, Sherratt MJ, Bay BK. A review of techniques for visualising soft tissue microstructure deformation and quantifying strain Ex Vivo. J Microsc. 2018;272:165-79.
[23] Brunon A, Bruyère-Garnier K, Coret M. Characterization of the nonlinear behaviour and the failure of human liver capsule through inflation tests.

Journal of the Mechanical Behavior of Biomedical Materials. 2011;4:1572-81.
[24] Elliott DM, Narmoneva DA, Setton LA. Direct Measurement of the Poisson's Ratio of Human Patella Cartilage in Tension. Journal of Biomechanical Engineering. 2002;124:223-8.
[25] Coudrillier B, Tian J, Alexander S, Myers KM, Quigley HA, Nguyen TD. Biomechanics of the Human Posterior Sclera: Age- and Glaucoma-Related Changes Measured Using Inflation TestingScleral Biomechanical Changes with Age/Glaucoma. Investigative Ophthalmology & Visual Science. 2012;53:1714-28.
[26] Kelleher JE, Zhang K, Siegmund T, Chan RW. Spatially varying properties of the vocal ligament contribute to its eigenfrequency response. Journal of the mechanical behavior of biomedical materials. 2010;3:600-9.
[27] Luyckx T, Verstraete M, De Roo K, De Waele W, Bellemans J, Victor J. Digital image correlation as a tool for three-dimensional strain analysis in human tendon tissue. Journal of Experimental Orthopaedics. 2014;1:7.
[28] Evans SL, Holt CA. Measuring the mechanical properties of human skin in vivo using digital image correlation and finite element modelling. The Journal of Strain Analysis for Engineering Design. 2009;44:337-45.
[29] Ottenio M, Tran D, Ní Annaidh A, Gilchrist MD, Bruyère K. Strain rate and anisotropy effects on the tensile failure characteristics of human skin. Journal of the Mechanical Behavior of Biomedical Materials. 2015;41:241-50.
[30] Sakaguchi R, Ferracane J, Powers J. Fundamentals of materials science. Craig's restorative dental materials. 14 ed: Elservier; 2019. p. 29-65.
[31] Lu H, Cary P. Deformation measurements by digital image correlation: implementation of a second-order displacement gradient. Experimental mechanics. 2000;40:393-400.
[32] Fitch AJ, Kadyrov A, Christmas WJ, Kittler J. Fast robust correlation. IEEE Transactions on Image Processing. 2005;14:1063-73.
[33] Poissant J, Barthelat F. A novel "subset splitting" procedure for digital image correlation on discontinuous displacement fields. Experimental mechanics. 2010;50:353-64.
[34] Lucas BD, Kanade T. An iterative image registration technique with an application to stereo vision. 1981.
[35] Bruck H, McNeill S, Sutton MA, Peters W. Digital image correlation using Newton-Raphson method of partial differential correction. Experimental mechanics. 1989;29:261-7.

[36] Cheng P, Sutton MA, Schreier HW, McNeill SR. Full-field speckle pattern image correlation with B-spline deformation function. Experimental mechanics. 2002;42:344-52.
[37] Sorzano COS, Thévenaz P, Unser M. Elastic registration of biological images using vector-spline regularization. IEEE Transactions on Biomedical Engineering. 2005;52:652-63.
[38] Bruck HA, McNeill SR, Sutton MA, Peters WH. Digital image correlation using Newton-Raphson method of partial differential correction. Experimental Mechanics. 1989;29:261-7.
[39] Ferracane JL, Hilton TJ. Polymerization stress – Is it clinically meaningful? Dental Materials. 2016;32:1-10.
[40] Ferracane JL. Developing a more complete understanding of stresses produced in dental composites during polymerization. Dental Materials. 2005;21:36-42.
[41] de Gee AF, Feilzer AJ, Davidson CL. True linear polymerization shrinkage of unfilled resins and composites determined with a linometer. Dent Mater. 1993;9:11-4.
[42] Park SH, Krejci I, Lutz F. Consistency in the amount of linear polymerization shrinkage in syringe-type composites. Dent Mater. 1999;15:442-6.
[43] Dennison JB, Yaman P, Seir R, Hamilton JC. Effect of variable light intensity on composite shrinkage. J Prosthet Dent. 2000;84:499-505.
[44] LEE IB, CHO BH, SON HH, UM CM. 벌크수축측정A new method to measure the polymerization shrinkage kinetics of light cured composites. Journal of Oral Rehabilitation. 2005;32:304-14.
[45] Labella R, Lambrechts P, Van Meerbeek B, Vanherle G. Polymerization shrinkage and elasticity of flowable composites and filled adhesives. Dental Materials. 1999;15:128-37.
[46] Rajan G, Raju R, Jinachandran S, Farrar P, Xi J, Prusty BG. Polymerisation Shrinkage Profiling of Dental Composites using Optical Fibre Sensing and their Correlation with Degree of Conversion and Curing Rate. Sci Rep. 2019;9:3162.
[47] Sharp LJ, Choi IB, Lee TE, Sy A, Suh BI. Volumetric shrinkage of composites using video-imaging. Journal of Dentistry. 2003;31:97-103.
[48] Chuang SF, Chen TY, Chang CH. Application of Digital Image Correlation Method to Study Dental Composite Shrinkage. Strain. 2008;44:231-8.

[49] Li J, Fok AS, Satterthwaite J, Watts DC. Measurement of the full-field polymerization shrinkage and depth of cure of dental composites using digital image correlation. Dent Mater. 2009;25:582-8.
[50] Li J-y, Lau A, Fok AS. Application of digital image correlation to full-field measurement of shrinkage strain of dental composites. Journal of Zhejiang University SCIENCE A. 2013;14:1-10.
[51] Li J, Thakur P, Fok AS. Shrinkage of dental composite in simulated cavity measured with digital image correlation. JoVE (Journal of Visualized Experiments). 2014:e51191.
[52] Kleverlaan CJ, Feilzer AJ. Polymerization shrinkage and contraction stress of dental resin composites. Dent Mater. 2005;21:1150-7.
[53] Li J, Li H, Fok AS, Watts DC. Multiple correlations of material parameters of light-cured dental composites. Dental Materials. 2009;25:829-36.
[54] Chuang S-F, Chang C-H, Chen TY-F. Spatially resolved assessments of composite shrinkage in MOD restorations using a digital-image-correlation technique. Dental Materials. 2011;27:134-43.
[55] Chuang SF, Chang CH, Chen TY. Contraction behaviors of dental composite restorations--finite element investigation with DIC validation. J Mech Behav Biomed Mater. 2011;4:2138-49.
[56] Chuang SF, Huang PS, Chen TY, Huang LH, Su KC, Chang CH. Shrinkage behaviors of dental composite restorations-The experimental-numerical hybrid analysis. Dent Mater. 2016;32:e362-e73.
[57] Chen TY-F, Huang P-S, Chuang S-F. Modeling dental composite shrinkage by digital image correlation and finite element methods. Optics and Lasers in Engineering. 2014;61:23-30.
[58] Lau A, Li J, Heo YC, Fok A. A study of polymerization shrinkage kinetics using digital image correlation. Dental Materials. 2015;31:391-8.
[59] Novaes Jr JB, Talma E, Las Casas EB, Aregawi W, Kolstad LW, Mantell S, et al. Can pulpal floor debonding be detected from occlusal surface displacement in composite restorations? Dental Materials. 2018;34:161-9.
[60] Martinsen M, El-Hajjar RF, Berzins DW. 3D full field strain analysis of polymerization shrinkage in a dental composite. Dent Mater. 2013;29:e161-7.
[61] Miletic V, Manojlovic D, Milosevic M, Mitrovic N, Stankovic TS, Maneski T. Analysis of local shrinkage patterns of self-adhering and flowable composites using 3D digital image correlation. Quintessence Int. 2011;42:797-804.
[62] Miletic V, Peric D, Milosevic M, Manojlovic D, Mitrovic N. Local

deformation fields and marginal integrity of sculptable bulk-fill, low-shrinkage and conventional composites. Dental materials. 2016;32:1441-51.
[63] Huang S-H, Lin L-S, Rudney J, Jones R, Aparicio C, Lin C-P, et al. A novel dentin bond strength measurement technique using a composite disk in diametral compression. Acta Biomaterialia. 2012;8:1597-602.
[64] Carrera CA, Chen Y-C, Li Y, Rudney J, Aparicio C, Fok A. Dentin-composite bond strength measurement using the Brazilian disk test. Journal of dentistry. 2016;52:37-44.
[65] Li Y, Carrera C, Chen R, Li J, Lenton P, Rudney JD, et al. Degradation in the dentin–composite interface subjected to multi-species biofilm challenges. Acta biomaterialia. 2014;10:375-83.
[66] Palamara J, Wilson P, Thomas C, Messer H. A new imaging technique for measuring the surface strains applied to dentine. Journal of dentistry. 2000;28:141-6.
[67] Wang W, Roubier N, Puel G, Allain J-M, Infante IC, Attal J-P, et al. A New Method Combining Finite Element Analysis and Digital Image Correlation to Assess Macroscopic Mechanical Properties of Dentin. Materials (Basel, Switzerland). 2015;8:535-50.
[68] Zhang D, Mao S, Lu C, Romberg E, Arola D. Dehydration and the dynamic dimensional changes within dentin and enamel. dental materials. 2009;25:937-45.
[69] Ivancik J, Arola DD. The importance of microstructural variations on the fracture toughness of human dentin. Biomaterials. 2013;34:864-74.
[70] Lu X, Rawson SD, Withers PJ. Effect of hydration and crack orientation on crack-tip strain, crack opening displacement and crack-tip shielding in elephant dentin. Dent Mater. 2018;34:1041-53.
[71] Zhang D, Luo M, Arola D. Displacement/strain measurements using an optical microscope and digital image correlation. Optical Engineering - OPT ENG. 2006;45.
[72] Sui T, Lunt AJ, Baimpas N, Sandholzer MA, Li T, Zeng K, et al. Understanding nature’s residual strain engineering at the human dentine–enamel junction interface. Acta biomaterialia. 2016;32:256-63.
[73] Lunt AJG, Chater P, Kleppe A, Baimpas N, Neo TK, Korsunsky AM. Residual strain mapping through pair distribution function analysis of the porcelain veneer within a yttria partially stabilised zirconia dental prosthesis. Dent Mater. 2019;35:257-69.
[74] Lu X, Fernández MP, Bradley RS, Rawson SD, O'Brien M, Hornberger B, et al. Anisotropic crack propagation and deformation in dentin observed

by four-dimensional X-ray nano-computed tomography. Acta Biomaterialia. 2019;96:400-11.
[75] Zhang D, Nazari A, Soappman M, Bajaj D, Arola D. Methods for examining the fatigue and fracture behavior of hard tissues. Experimental Mechanics. 2007;47:325-36.
[76] Zhang D, Lu C, Zhang X, Mao S, Arola D. Contact fracture of full-ceramic crowns subjected to occlusal loads. Journal of Biomechanics. 2008;41:2995-3001.
[77] Jiang Y, Akkus A, Roperto R, Akkus O, Li B, Lang L, et al. Measurement of J-integral in CAD/CAM dental ceramics and composite resin by digital image correlation. Journal of the mechanical behavior of biomedical materials. 2016;62:240-6.
[78] Soares Porto T, Roperto R, Akkus A, Akkus O, Porto-Neto S, Teich S, et al. Mechanical properties and DIC analyses of CAD/CAM materials. 2016.
[79] Sebastiani M, Massimi F, Merlati G, Bemporad E. Residual micro-stress distributions in heat-pressed ceramic on zirconia and porcelain-fused to metal systems: Analysis by FIB–DIC ring-core method and correlation with fracture toughness. Dental Materials. 2015;31:1396-405.
[80] Chen D, Carter E, Kamlah M. Deformation behavior of lead zirconate titanate ceramics under uniaxial compression measured by the digital image correlation method. Smart Materials and Structures. 2016;25:097001.
[81] Choi B-J, Yoon S, Im Y-W, Lee J-H, Jung H-J, Lee H-H. Uniaxial/biaxial flexure strengths and elastic properties of resin-composite block materials for CAD/CAM. Dental Materials. 2019;35:389-401.
[82] Ni C-W, Chang C-H, Chen TY-F, Chuang S-F. A multiparametric evaluation of post-restored teeth with simulated bone loss. Journal of the mechanical behavior of biomedical materials. 2011;4:322-30.
[83] Tiossi R, Lin L, Conrad HJ, Rodrigues RC, Heo YC, de Mattos MdGC, et al. A digital image correlation analysis on the influence of crown material in implant-supported prostheses on bone strain distribution. Journal of prosthodontic research. 2012;56:25-31.
[84] Tiossi R, Lin L, Rodrigues RC, Heo YC, Conrad HJ, Maria da Gloria C, et al. Digital image correlation analysis of the load transfer by implant-supported restorations. Journal of biomechanics. 2011;44:1008-13.
[85] Tiossi R, de Torres EM, Rodrigues RC, Conrad HJ, de Mattos Mda G, Fok AS, et al. Comparison of the correlation of photoelasticity and digital imaging to characterize the load transfer of implant-supported restorations. J Prosthet Dent. 2014;112:276-84.

[86] Tiossi R, Vasco MA, Lin L, Conrad HJ, Bezzon OL, Ribeiro RF, et al. Validation of finite element models for strain analysis of implant-supported prostheses using digital image correlation. Dent Mater. 2013;29:788-96.
[87] Tribst JPM, Dal Piva AMO, Bottino MA, Nishioka RS, Borges ALS, Ozcan M. Digital Image Correlation and Finite Element Analysis of Bone Strain Generated by Implant-Retained Cantilever Fixed Prosthesis. Eur J Prosthodont Restor Dent. 2020;28:10-7.
[88] Alhamdan MM, Knowles JC, McDonald A. Digital Image Correlation and Strain Gauges to Map and Compare Strain in Teeth with Different Quantity and Quality of Remaining Tooth Structure. Int J Prosthodont. 2019;32:82-90.
[89] Tiossi R, Gomes EA, Faria ACL, Rodrigues RCS, Ribeiro RF. Biomechanical behavior of titanium and zirconia frameworks for implant-supported full-arch fixed dental prosthesis. Clin Implant Dent Relat Res. 2017;19:860-6.
[90] Tanasic I, Milic-Lemic A, Tihacek-Sojic L, Stancic I, Mitrovic N. Analysis of the compressive strain below the removable and fixed prosthesis in the posterior mandible using a digital image correlation method. Biomech Model Mechanobiol. 2012;11:751-8.
[91] Tanasic I, Tihacek-Sojic L, Milic-Lemic A. Biomechanical behavior of restored and unrestored mandible with shortened dental arch under vertical loading condition. Acta Bioeng Biomech. 2012;14:31-6.
[92] Clelland NL, Yilmaz B, Seidt JD. Three-Dimensional Image Correlation Analyses for Strains Generated by Cement and Screw-Retained Implant Prostheses. Clinical implant dentistry and related research. 2013;15:271-82.
[93] Calha N, Messias A, Guerra F, Martinho B, Neto MA, Nicolau P. Effect of geometry on deformation of anterior implant-supported zirconia frameworks: An in vitro study using digital image correlation. Journal of prosthodontic research. 2017;61:139-48.
[94] Yilmaz B, Mess J, Seidt J, Clelland NL. Strain comparisons for splinted and nonsplinted cement-retained implant crowns. International Journal of Prosthodontics. 2013;26.
[95] Clelland NL, Yilmaz B, Seidt JD. Three-dimensional image correlation analyses for strains generated by cement and screw-retained implant prostheses. Clin Implant Dent Relat Res. 2013;15:271-82.
[96] Yilmaz B, Hashemzadeh S, Seidt JD, Clelland NL. Displacement comparison of CAD–CAM titanium and zirconia abutments to implants with different conical connections. Journal of prosthodontic research. 2018;62:200-3.

[97] Salaita LG, Yilmaz B, Seidt JD, Clelland NL, Chien HH, McGlumphy EA. Strain analysis of 9 different abutments for cement-retained crowns on an internal hexagonal implant. J Prosthet Dent. 2017;118:166-71.
[98] de Carvalho EB, Herbst PE, Faria ACL, Ribeiro RF, Costa PP, Tiossi R. Strain transfer behavior of different planning options for mandibular single-molar replacement. J Prosthet Dent. 2018;119:250-6.